

Morning session

1. Keynote:

First Observation of Superradiant Tera Hertz Radiation at the Israeli Free Electron Laser

A. Friedman, A. Gover*, A. Nause, Y. Vashdi, P. Ben Ishai, E. Dyunin, Y. Lurie, D. Borodin, A. Yahalom, A. Weinberg, A. Haj Yehye, E. Farchi

Ariel University, Dept. of Electrical Engineering, Schlesinger Center for Compact Accelerator

*Tel Aviv University, Dept. of Physical Electronics, Israeli FEL Center

We report the first measurement of Tera Hertz light at the Israeli FEL facility. This facility is based on the ORGAD accelerator (Optically-driven RF Gun Accelerator Development), a 3 – 8.5 MeV compact accelerator hybrid gun (63 cm). The FEL is based on our innovative concept of bunched beam superradiance - enhanced coherent radiation by an electron beam bunched to less than a radiation wavelength. The bunching is facilitated by introducing chirp into the electron pulse at the gun. The pulse then contracts as it traverses a drift section of 6 meters. It arrives at the undulator magnet with a length of less than 100 femto seconds. This results in generation of spontaneous emission at the undulator where all the electrons are in phase. Because of this, the electromagnetic fields generated by various electrons add up, resulting in an emission proportional to the square of the number of electrons. In comparison, the radiation of regular spontaneous emission is proportional to the number of electrons. Thus, the energy emitted per pulse is enhanced by a factor of the number of electrons (X108 for the case of $Q=20\text{pC}$) without stimulated emission.

With the present beam parameters, the radiation is emitted at frequency of 3.5 THz in 12 picS long pulses of radiative energy in excess of 350 nano-Joule per pulse.

This work was supported in parts by MoD, MoS and ISF.

This work is dedicated to the memories of Yigal Cohen Orgad and Demitry Borodin.

2.

Disruptions in the ITER Tokamak

H. Strauss¹

¹ HRS Fusion, Jerusalem, Israel

Disruptions occur in nearly all tokamaks. They cause a thermal quench (TQ), in which the plasma energy is lost, followed a current quench. In present tokamaks, these events occur in milliseconds. In large future magnetic fusion devices, this would cause an unacceptable heat and electro mechanical load. Not to worry! It was recently found [1,2,3] that disruptions are caused by resistive wall tearing modes (RWTM). These are tearing instabilities which have a resonant surface close enough to the conducting wall surrounding the plasma to have a strong effect. If the wall is a perfect conductor, the tearing mode is stable, but if there is no wall, the RWTM is unstable. If the wall has some resistivity, the RWTM grows on a timescale dependent on the wall resistive penetration time. This is shown in Fig. 1. The ITER and MST values are based on MHD

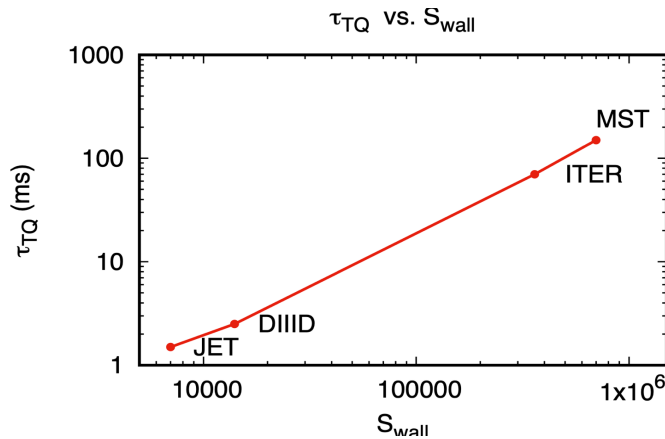


Fig. 1 shows thermal quench time for several experiments. The horizontal scale is the resistive wall penetration time normalized to Alfvén time. The vertical

simulations, while JET and DIIIID times are experimental data.

[1] H. Strauss, Phys. Plasmas 28, 072507 (2021)

[2] H. Strauss, B. C. Lyons, M. Knolker, Phys. Plasmas 29, 112508 (2023)

[3] H. Strauss, B. E. Chapman, to be submitted

3.

Fast solid-state switches at Soreq NRC

A. S. Kesar, D. Cohen-Elias, G. Atar, S. Zoran, A. Raizman, M. Wolf, and M. Katz

Solid-State Physics Department, Applied Physics Division, Soreq NRC, Israel

Fast silicon solid-state switches are designed and fabricated at the Soreq Nuclear Research Center (NRC). Fast silicon-controlled rectifier (SCR) was designed as a five-layer structure, with a thick ($>500\ \mu\text{m}$) intrinsic layer for a high-voltage operation. When operated in a characterization circuit, we demonstrated a switching of 2.7 kV, 1.8 kA, at a speed of less than 300 ns [1]. The cathode area was $3.25\ \text{mm}^2$, resulting in a current density of $55\ \text{kA/cm}^2$. This fast SCR is intended to serve as a primary switch for driving a drift-step recovery diode (DSRD).

The DSRD is a fast, 1-ns, current interruption switch. When used along with an inductor, a high-voltage pulse commutes into a load. Traditional designs rely on deep diffusion processes for a four-layer structure, which complicates its fabrication. We present a three-layer structure based on a thick, $70\text{-}\mu\text{m}$ layer, by epitaxial growth process. This results in a simplified fabrication process, which fits for production in regular fabs. We demonstrated a 1-kV operation by a single DSRD die, with a voltage rise-rate of $0.8\ \text{kV/ns}$, and 31.6 kV with a rise-time of 2.7 ns by a stack of diodes [2]. The load was $50\ \Omega$. This pulsed is used to drive a fast-avalanche diode.

The fast-avalanche diode is a fast, 100-ps, closing switch. We present a three-layer structure based on a thick ($>500\ \mu\text{m}$) high-resistivity Si-wafer. This design eliminates fabrication process difficulties such as deep diffusion or thick epitaxial layers. State-of-the-art results of 8-kV, 100-ps rise-time, with a voltage rise-rate of 57-kV/ns were obtained from a single, 4-mm^2 die. A pulse of 46-kV with a voltage rise-rate of 192-kV/ns was measured by a stack made of five, 8-mm^2 dies. The load was $50\ \Omega$ [3].

The circuit topology relies on pulse compression by these type of switches along with air-coils, which makes it relatively compact. A 29.5 kV pulse with a rise time of 238-ps was obtained by cascading two DSRD stages and two fast-avalanche diodes. The circuit volume was 3.5 liters [2]. It included the Soreq NRC diodes and a commercial primary switch. The latter is intended to be replaced by our SCR.

[1] D. Cohen-Elias, A. S. Kesar, S. Zoran, G. Atar, M. Katz, A. Raizman, "Fast silicon controlled rectifier for driving nanosecond-scale high-voltage pulses circuits," The 35th International Symposium on Power Semiconductor Devices and ICs, 2023, submitted.

[2] Amit S. Kesar, Michael Wolf, Arie Raizman, and Shoval Zoran, "A 30-kV, 240-ps rise-time pulsed-power circuit by an epi-Si drift-step-recovery diode and a fast-avalanche diode," IEEE Transactions on Plasma Science, submitted.

[3] Amit S. Kesar, Arie Raizman, Gil Atar, Shoval Zoran, Svetlana Gleizer, Yakov Krasik, and Doron Cohen-Elias, "A fast avalanche Si diode with a $517\ \mu\text{m}$ low-doped region," Applied Physics Letters, **117**, 013501, (2020).

4.

Supersonic water jets as point-like sources of extremely high pressure

¹D. Maler, ¹R. Grikshtas, ¹S. Efimov, ¹L. Merzlikin, ²M. Liverts ³M. Kozlov, ⁴J. Strucka, ⁴Y. Yao, ⁴K. Mighal, ⁵A. Rack, ⁵B. Lukic, ⁴S. N. Bland and ¹Ya. E. Krasik

¹Physics Department, Technion, Israel Institute of Technology, Haifa 3200003, Israel

²Engineering Mechanics Department, Royal Institute of Technology, Stockholm 114 28, Sweden

³Nazarbayev University, Nur-Sultan 010000, Kazakhstan

⁴Plasma Physics Group, Imperial College London, London SW7 2BW, United Kingdom

⁵European Synchrotron Radiation Facility, CS40220, 38043 Grenoble Cedex 9, France

Results of experimental research and numerical simulations related to the application of supersonic water jets, generated by the underwater electrical explosion (UEWE) of axially symmetric wire arrays, for the study of high energy density physics are presented. In experiments, we used two configurations to (1) study the interaction of two counter-streaming water jets in a capsule filled with air and (2) the interaction of a water jet with a metal target of various thicknesses. Experimental results were either compared to two dimensional hydrodynamic simulations, reproducing measured quantities, or, using the simulation, estimating the state of water where optical probing does not allow one to infer on the state of water. These numerical results showed that for water jets propagating with initial velocity of ~ 2 km/s, water and target parameters can reach ~ 20 - 30 GPa, temperatures of ~ 2000 K and significant material compression. Scaling the experimental setup with larger and faster pulse power systems predict extreme states of matter, exceeding energy densities of > 100 GPa.

The Propagation of Ultra-Wideband Modulated Pulses in Plasma Media

Yosef Golovachev¹, Gad A. Pinhasi² and Yosef Pinhasi³

¹Dept. of Electrical and Electronic Engineering

The Jerusalem College of Technology, P.O. Box 16031, Jerusalem 91160, ISRAEL

²Dept. of Chemical Engineering ³Dept. of Electrical and Electronic Engineering,

Ariel University, P.O. Box 3, Ariel 40700, ISRAEL

Electromagnetic (EM) propagation in plasma media is one of the most challenging issues in modern EM theory. Previous works [1], [2], [3], [4] have studied the general EM propagation in plasma media. The presented research focuses on the propagation of ultra-wideband modulated pulses in plasma while considering absorptive and dispersive effects (see Figure 1). Ultra-short pulses are used in high data-rate digital wireless communications, high-resolution radars as well as in spread-spectrum techniques.

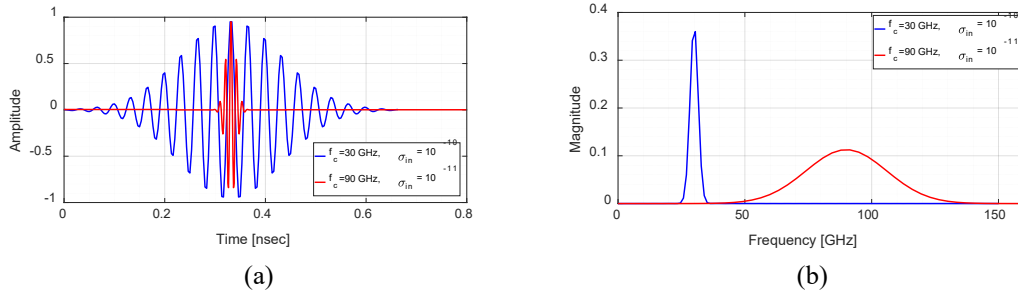


Figure 1.

Modulated Gaussian Pulse in (a) time domain and (b) frequency domain.

We consider a carrier wave centered at a frequency f_c . The carrier is modulated by a wideband signal:

$$E_{in}(t) = \text{Re}\{A_{in}(t)e^{j2\pi f_c t}\} \quad (1)$$

where $A_{in}(t)$ is a complex envelop, representing the baseband modulating signal. In the analysis, we assume that the transmitted signal is modulated by a Gaussian envelope [5]:

$$A_{in}(t) = e^{-\frac{t^2}{2\sigma_{in}^2}} \quad (2)$$

where σ_{in}^2 is a standard deviation of Gaussian distribution. The frequency dependent plasma electric permittivity [6],[7] is given by:

$$\varepsilon_r(f) = 1 - \frac{f_p^2}{f^2 + f_e^2} - j \frac{f_e}{f} \frac{f_p^2}{f^2 + f_e^2} \quad (3)$$

where f_p is the plasma frequency and f_e is electron collision frequency. Its real and imaginary parts are $\varepsilon_r'(f)$ and $\varepsilon_r''(f)$, respectively. The propagation factor of the EM wave is expressed via the dielectric medium properties

$k(f) = 2\pi f \sqrt{\varepsilon_r(f)} / c$, where c is the speed of light in vacuum. The imaginary part of propagation factor is the attenuation coefficient $\alpha(f) = -\text{Im}[k(f)]$. The real part of propagation factor $\beta(f) = \text{Re}[k(f)]$ is the phase dispersion of the wave propagating in the medium [7]:

$$\alpha(f) = -\text{Im}\{k(f)\} = \frac{2\pi f}{c} \sqrt{\frac{\varepsilon_r'(f)}{2} \left[\sqrt{1 + \left(\frac{\varepsilon_r''(f)}{\varepsilon_r'(f)}\right)^2} - 1 \right]} \left[\frac{1}{m} \right] \quad (4)$$

$$\beta(f) = \text{Re}\{k(f)\} = \frac{2\pi f}{c} \sqrt{\frac{\varepsilon_r'(f)}{2} \left[\sqrt{1 + \left(\frac{\varepsilon_r''(f)}{\varepsilon_r'(f)}\right)^2} + 1 \right]} \left[\frac{\text{rad}}{m} \right] \quad (5)$$

Propagating along a distance d in the plasma medium, the electronic field of the wave is:

$$E_{out}(t) = \text{Re}\{A_{out}(t)e^{j2\pi f_c t}\} \quad (6)$$

where $A_{out}(t)$ is a complex envelop of the signal at the output:

$$A_{out}(t) = \frac{\sigma_{in}}{\sigma} e^{-\frac{t^2}{2\sigma_{out}^2}} \quad (7)$$

In this study we describe an analytical model for estimating the power attenuation, propagation delay and the spread of ultra-wideband modulated pulses in different plasma media.

References

- [1] D. Kalluri and R. K. Shrivastava, "Reflection and transmission of electromagnetic waves obliquely incident on a relativistically moving isotropic plasma slab," *J. Appl. Phys.*, vol. 44, no. 5, May 1972, Art. no. 2440.
- [2] C. Yeh and K. F. Casey, "Reflection and transmission of electromagnetic waves by a moving dielectric slab," *Phys. Rev.*, vol. 144, pp. 665–669, Apr. 1966.
- [3] D. Kalluri and R. K. Shrivastava, "Reflection and transmission of electromagnetic waves obliquely incident on a relativistically moving uniaxial plasma slab," *IEEE Trans. Antennas Propag.*, vol. AP-21, no. 1, pp. 63–70, Jan. 1973.
- [4] P. Daly and H. Gruenberg, "Energy relations for plane waves reflected from moving media," *J. Appl. Phys.*, vol. 38, pp. 4486–4489, Jul. 1967.
- [5] Pinhasi, Y., Yahalom, A., and Pinhasi, G. A. (2009). Propagation analysis of ultrashort pulses in resonant dielectric media. *J. Opt. Soc. Am. B*, 26(12), 2404-2413.
- [6] Gibbon, P. 2020 *Introduction to Plasma Physics*. Forschungszentrum Jülich GmbH, Institute for Advanced Simulation, Jülich Supercomputing Centre, Jülich, Germany.
- [7] Ginzburg, V.L. 1961. *Propagation of electromagnetic waves in plasma*. New York: Gordon and Breach Science Publishers, ISBN-10: 0677200803, 822 pp.

6.

RF plugging of multi-mirror machines

T. Miller^{1,2}, I. Be'ery², E. Gudinetsky¹, and I. Barth¹

¹Racah Institute of Physics, The Hebrew University of Jerusalem, Jerusalem, 91904

²Rafael Plasma Laboratory, Rafael Advanced Defense Systems, POB 2250, Haifa, 3102102
Israel

One of the main challenges of fusion reactors based on the linear magnetic mirror is the axial particle loss through the loss cones. The multi-mirror (MM) system addresses the particle loss by adding mirror cells on each end of the central fusion cell. Coulomb collisions in the MM sections serve as the retrapping mechanism for the escaping particles. Unfortunately, the confinement time in this system only scales linearly with the number of cells in the MM sections, which requires an unreasonably large number of cells to satisfy the Lawson criterion. Here, it is suggested to apply a traveling RF electric field that mainly targets the particles in the outgoing loss cone. The Doppler shift compensates for the detuning of the RF frequency from the ion cyclotron resonance mainly for the escaping particles resulting in a selectivity effect. The transition rates between the different phase space populations are quantified via single-particle calculations and then incorporated into a semi-kinetic rate equations model for the MM system, including the RF effect. It is found that the confinement time can scale exponentially with the number of MM cells, orders of magnitude better than a similar MM system with a reasonable length but without the RF plugging.

Afternoon session

7. Keynote:

The Physics of Field-reversed Configuration (FRC) Fusion Reactors

Samuel A. Cohen

Plasma Physics Laboratory, Princeton University, Princeton, NJ 08543, United States

In contrast to the mainline magnetic fusion devices, tokamaks and stellarators, FRCs have high β (ratio of plasma-energy density to magnetic-field energy density), no azimuthal magnetic field, and a quasi-linear geometry. These provide substantial technological benefits but also require new physics insights and approaches to understand an FRC's behavior and to optimize an FRC reactor's design. Critical FRC plasma properties are stability and transport. These will impact choices made for an FRC reactor's size, fuel, and heating method. In this talk I will describe three contrasting approaches to FRC design and the status of research in each.

8.

On the interaction of hydrogen with ceria in ambient conditions: hydride formation VS hydroxylation of the surface

Adva Ben-Yaacov¹, Roey Ben-David¹, Lorentz Falling², Slavomir Nemsak² and Baran Eren^{1*}

¹Department of Chemical and Biological Physics, Weizmann Institute of Science, 234 Herzl Street, 76100 Rehovot, Israel,

²Advanced Light Source, Lawrence Berkeley National Laboratory, Berkeley, California 94720, United States

Ceria catalysts present a great potential for the selective hydrogenation of alkynes to alkenes and the hydrogenation of CO₂ to methanol [1]. Recent works suggest that the type of surface and subsurface hydrogen may play an important role, affecting both the activity and the selectivity in hydrogenation reactions. Interaction with hydrogen go typically through two routes: homolytic dissociation to form two hydroxyls and heterolytic route to form hydride and a proton, although other pathways are possible. The hydrides are stabilized by oxidizing the cerium atoms next to the oxygen vacancies [2,3].

Using simultaneous X-ray photoelectron spectroscopy (XPS), X-ray absorption spectroscopy, and grazing incidence resonant X-ray scattering (GIXS) measurements at ambient conditions, we aim to understand both the structural and chemical changes occurring during reduction, oxidation, and interaction with hydrogen. We measured resonant X-ray scattering at Ce M₅ edge to distinguish between Ce⁴⁺ or Ce³⁺ species revealing dramatic changes in shape of the form factor. X-ray photoelectron spectroscopy shows that the surface was most oxidized when annealed in the H₂ atmosphere, suggesting formation of hydrides. Ceria can expand through the process, and this volumetric change can be observed in diffraction measurements. Correlation of all the simultaneously acquired spectral and diffraction data gains novel insights of the ceria-H₂ system.

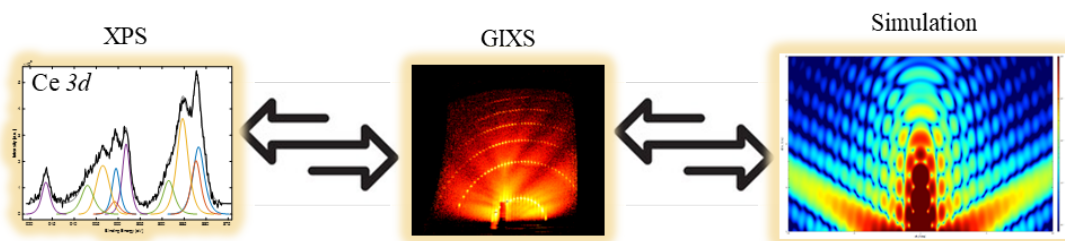


Fig. 1: Schematic representation of the experiment process combining chemical information from XPS, structural information from GIXS and simulation of GIXS images with XPS as an input.

- [1] J. A. R. Jesús Graciani, K. Mudiyansele, F. Xu, A. E. Baber, J. Evans, S. D. Senanayake, D. J. Stacchiola, P. Liu, J. Hrbek, J. Fernández Sanz and J. A. Rodrigues, *Science*, 345, 546 (2014).
- [2] Z. Li, K. Werner, L. Chen, A. Jia, K. Qian, J. Q. Zhong, R. You, L. Wu, L. Zhang, H. Pan, X. P. Wu, X. Q. Gong, S. Shaikhutdinov, W. Huang, H. J. Freund, *Chem. - A Eur. J.*, 27, 16, 5268, (2021).
- [3] D. Schweke, L. Shelly, R. Ben David, A. Danon, N. Kostirya, and S. Hayun. *J. Phys. Chem. C*, 124, 11, 6180, (2020).

9.

Autoresonant ash removal in magnetic mirrors

E. Gudinetsky^{1,2}, I. Be'ery³, T. Miller^{1,3}, and I. Barth¹

¹Racah Institute of Physics, The Hebrew University of Jerusalem, Jerusalem, 91904

²Department of Physics, Nuclear Research Center, Negev, PO Box 9001, Beer Sheva, Israel

³Rafael Plasma Laboratory, Rafael Advanced Defense Systems, POB 2250, Haifa, 3102102
Israel

The design of future magnetic confinement fusion reactors must account for managing the fusion by-products (ash) by either utilizing them for power generation or discarding them to increase fusion efficacy. The present study focuses on linear magnetic mirror-type reactors, in which an inhomogeneous magnetic field contains both fuel and ash particles, albeit some particles may escape through the loss cone or by radial instabilities. It is proposed to exploit the autoresonance phenomenon to discard trapped ash particles through the loss cone. The ash particles are resonantly driven by a small perturbation to the axial magnetic field with chirped frequency. As a result, the phase-locked ash particles increase their axial velocity until they escape outside the reactor through the loss cone. Monte Carlo simulations are used to quantify the ash removal efficiency. Notably, the time scale difference ensures that the fuel particles are not resonant and therefore do not escape the system.

10.

Reactive Sputtering of Nickel Nitride passivation layers Improves Halide Perovskite P-I-N Solar cells

Anat Itzhak,¹ Xu He,² Adi Kama,¹ Sujit Kumar,^{1,3} Michal Ejgenberg,¹ Antoine Kahn,² David Cahen^{1,3}

¹ Department of Chemistry, Center for Nanotechnology & Advanced Materials, Bar Ilan University, 5290002 Ramat Gan, Israel

² Department of Electrical and Computer Engineering, Princeton University, Princeton, New Jersey, 08544, United States

³ Weizmann Institute of Science, Rehovot 76100

Stability is one of the significant barriers to commercializing halide perovskite, HaP, devices. The interfaces between inorganic selective contacts and halide perovskites (HaPs) are the greatest challenge for making stable and reproducible devices with these materials. Nickel oxide (NiO_x) is an attractive hole-transport layer as it fits the electronic structure of HaPs, is highly durable, and can be produced at a low cost. In this work, we deposited highly controlled NiO_x layers using RF sputtering, followed by a reactive in-situ deposition of an ultra-thin nickel nitride (Ni_yN) passivation layer. We used Ar plasma etching to polish the Ni_yN layer, so it will be thin enough to retain charge transfer and continuous enough to protect NiO_x and maintain its conductivity.

The Ni_yN buffer layer passivating the interface between NiO_x and the HaPs and protects the HaP from the reactive Ni^{+3} species in the NiO_x layer. This double effect of the Ni_yN layer improves PSCs efficiency from an average of 16.5% to 19% and increases the device stability, as exhibited by measurements over four days. Using RF sputtering to deposit inorganic passivation layers is an innovative step towards a scalable process of stable HaP-based solar cells.

11.

Diamond characterization via microwave spectroscopy

Y. Rabinowitz¹, Y. Pinhasi¹, A. Yahlom¹ and H. Cohen²

¹Department of Electrical Engineering, Ariel University, Ariel, Israel

²Department of Chemical Studies, Ariel University, Ariel, Israel

Abstract

Two of the most important parameters affecting the price of natural colorless diamonds are: (i) its color grade. The range of color grades in the trade is denoted by alphabet letters from D to M, where D represents the best commercial quality. and (ii) is it a natural or lab grown diamond which much cheaper in price .

The color grade of diamonds is largely influenced by their nitrogen content (when nitrogen atoms substitute carbon atoms in the crystal) and can be determined from this property. Diamonds absorb electromagnetic radiation in the UV-visible and in the Infrared spectral range. Therefore, their color grade is measured via spectral light absorption in these wavelengths ranges.

However, increasing the range to the microwave region (higher wavelength) can be a new and more efficient method, as the effect of stray light is relative to $1/\lambda^4$, namely at higher wavelength the stray light will have much smaller interference.

The electromagnetic properties of different polished diamonds having several nitrogen concentrations in the frequency range of 100-110 GHz (W band) have been studied. The results indicate that there is a good correlation between the amount of nitrogen impurities and the Free Spectral Range (FSR) parameter of a reflection signal, S11, in the antenna. From the study, it is concluded that measuring the diamonds dielectric properties via spectroscopic analysis in the millimeter wavelength range, can determine the color grade parameter of the diamond. In addition, the FSR measurements were correlated well with the FTIR measurements and the GIA (Gemological Institute of America) reports.

The methodology of the new color determination mode and a novel color estimate, based on the FSR vs the nitrogen correlation, has been carried out with 26 diamonds with a success rate higher than 70%. The second parameter is the determination the source of the diamond: natural or synthetic- lab grown . The HPHT (High Pressure High Temperature) process produces diamonds; thus, there is a need in gemological laboratories to determine whether the diamond is natural or produced via the HPHT method.

A new analysis method based on microwave (MW) spectroscopy is proposed. Using the transmission/reflection method (TRM), we determine whether a diamond is natural or lab grown

via HPHT. Several waveguides, which cover the 12-26 GHz frequency range, were developed. A good correlation between the S12 parameter and the origin of the diamond was obtained. The results in the spectral range of 12-12.7GHz, 20.9-21 GHz, and 22.2-22.23 GHz suggest that this is an efficient method for determining whether a diamond is produced via the HPHT process, or it is a natural diamond.

The Rate of Dissipation of Generalized Cross Helicity and Magnetic Helicity in Non-ideal Magnetohydrodynamics – a Comparative Study

P. Sharma^{1,2} and A. Yahalom^{1,2}

¹Department of Electrical & Electronic Engineering, Ariel University, Ariel, Israel

² Center for Astrophysics, Geophysics, and Space Sciences (AGASS),

Ariel University, Ariel, Israel

The objective of the present presentation is to investigate the constancy of the topological invariants denoted non-barotropic generalized cross helicity in the case of non-ideal magnetohydrodynamic (MHD). In our previous works we considered only ideal barotropic MHD and ideal non-barotropic MHD. Here we consider dissipative processes in the form of thermal conduction, finite electrical conductivity and viscosity and the effect of these processes on the helicity conservation. Analytical approach has been adopted to obtain the mathematical expressions for the time derivative of helicity in a non-dimensional form showing the dependence of helicity dissipation on the Rayleigh and magnetic Rayleigh numbers. We also give a concrete model comparing the dissipation of magnetic and cross helicity and show that for small viscosity and heat conduction the rate of dissipation is comparable.

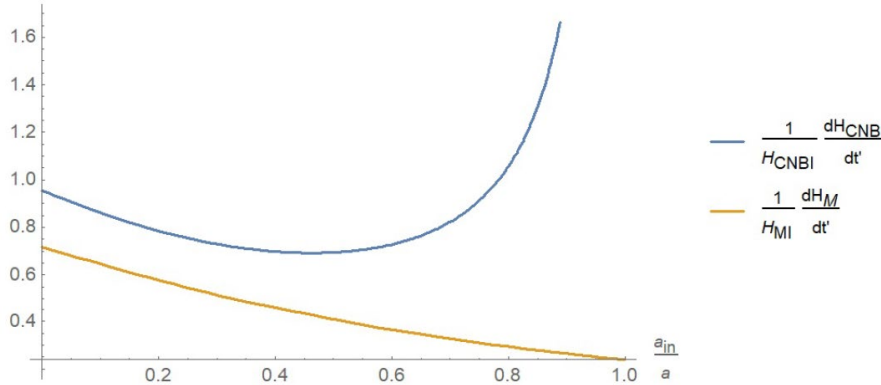


Fig. 1: Comparison $\left| \frac{1}{H_{MI}} \frac{dH_{MI}}{dt'} \right|$ and $\left| \frac{1}{H_{CNBI}} \frac{dH_{CNBI}}{dt'} \right|$ for $R_m = 1$

[1] Yahalom, A. (2017a). Geophysical & Astrophysical Fluid Dynamics, 111(2), 131–137.

[2] Yahalom, A. (2017b). Fluid Dynamics Research, 50(1), 011406.

[3] Yahalom, A., & Qin, H. (2021). Journal of Fluid Mechanics, 908.

[4] Sharma, P., Yahalom, A., (2022). arXiv:2207.12309 [physics.flu-dyn].